

1 **Influence of high-pressure homogenization on functional properties of orange**
2 **pulp**

3 *Sandy Van Buggenhout¹, Joël Wallecan², Stefanie Christiaens¹, Stephane J.J. Debon², Christina Desmet²,*
4 *Ann Van Loey¹, Marc Hendrickx^{1,*}, Jacques Mazoyer³*

5 ¹ Laboratory of Food Technology and Leuven Food Science and Nutrition Research Centre (LForCe),
6 Department of Microbial and Molecular Systems (M²S), KU Leuven, Kasteelpark Arenberg 22 box 2457,
7 3001 Heverlee, Belgium

8 ² Cargill R&D Centre Europe, Havenstraat 84, 1800 Vilvoorde, Belgium

9 ³ Cargill usine de Baupte, 50500 Carentan, France

10 *Corresponding author. Tel.: +32 16 32 15 72; fax: +32 16 32 19 60.

11 E-mail address: marc.hendrickx@biw.kuleuven.be

12 **Abstract**

13 The current work evaluated whether high-pressure homogenization (HPH) could functionalize orange
14 pulp in terms of water holding and swelling capacity and rheological properties. The orange pulp particle
15 size was gradually decreased by applying HPH at increasing pressure (200 and 800 bar) whereby the
16 mechanical impact at 800 bar resulted in the appearance of a more homogeneous, smoother suspension
17 with a twofold increase in yield stress. HPH also affected the pectin properties within the orange pulp
18 cell walls. More specifically, HPH at 800 bar increased the relative presence of water-extractable pectin.
19 By investigating subsamples containing particles with different sizes isolated from orange pulp before
20 and after HPH, it became clear that particle size is inversely related to the water holding capacity and
21 the ability of the particle network to deform prior to flow. Especially highly disintegrated orange pulp
22 material (< 40µm) contributes to the water holding capacity and the soft particle network behavior.

23 **Industrial relevance**

24 Orange pulp is of particular interest in the context of producing fiber-rich functional ingredients because
25 of its large quantity available within the juice industry. High-pressure homogenization (HPH) at
26 pressures higher than the ones usually applied in food industry seems required to functionalize orange
27 pulp as HPH at 200 bar (a common pressure applied in the food industry) could not increase the relative
28 presence of small particles, contributing to water holding capacity and soft particle network behavior, as
29 substantially compared to HPH at 800 bar.

30

31 **Keywords:** orange pulp, high-pressure homogenization, swelling volume, water holding capacity, pectin

32 **Abbreviations used**

33 AIR = alcohol-insoluble residue

34 CEC = cation exchange capacity

35 CEP = chelator-extractable pectin

36 DME = degree of methyl-esterification

37 FITC = fluorescein isothiocyanate

38 HF = hemicellulose fraction

39 HPH = high-pressure homogenization

- 40 LVE = linear viscoelastic
41 MM = molar mass
42 NEP = sodium carbonate-extractable pectin
43 OHC = oil holding capacity
44 PBS = phosphate buffered saline
45 UA = uronic acid
46 WHC = water holding capacity
47 WEP = water-extractable pectin

48

49 **1 Introduction**

50 Consumption of dietary fiber is linked to health benefits associated with bowel function, reduced risk of
51 coronary heart diseases and type 2 diabetes and weight management (Hauner et al., 2012).
52 Unfortunately, the average total dietary fiber consumption (14 to 29 g/day) is far below the
53 recommended intake between 21 and 40 g/day (WHO/FAO, 2003). This recommendation could be
54 achieved by increasing the consumption of fruits and vegetables: it is suggested to eat five to nine
55 pieces a day. On the other hand, fiber-enriched food products could also play a key role in our diet.
56 Fruit and vegetable by-products, mainly consisting of cell wall material rich in dietary fiber, can in this
57 context be considered as potentially interesting functional ingredients. In order to create healthy, fiber-
58 rich food products that consumers like to eat, functional food ingredients should not only possess
59 desired nutritional properties but also particular technological functional properties in terms of
60 hydration properties, surface activity and texturization. Compared to commonly-used hydrocolloid
61 ingredients, the structure-forming properties of plant cell wall-derived fibers, currently available on the
62 market, are however limited. Because of its large quantity available within the juice manufacturing
63 industry, orange pulp is of particular interest in the context of producing fiber-rich functional
64 ingredients. The limited functionality of orange pulp, when dispersed in water, however confines
65 valorization pathways for this by-product.

66 Mechanical processing is known to alter the physicochemical properties of plant-based fiber
67 suspensions. During mechanical processing, particle sizes are reduced to a certain micro-scale level
68 enhancing physicochemical properties such as the water holding capacity (WHC), the swelling capacity,

69 the oil holding capacity (OHC) and the cation exchange capacity (CEC). Mechanical processing
70 techniques based on high-pressure processes, e.g. high-pressure homogenization (HPH) and
71 microfluidization, have been shown more effective in particle size reduction compared to conventional
72 mechanical processing techniques such as ball milling and jet milling (Chau, Wang, & Wen, 2007). In
73 these high-pressure valve homogenizers, the fluid is forced through a small gap between seat and valve
74 creating elongational and turbulence stresses modifying the fluid. Alternative technologies such as
75 steam explosion and supercritical CO₂ explosion have also demonstrated the ability to open up the
76 structures of plant based biomasses (Tanahashi, 1990; Narayanaswamy, Faik, Goetz, & Gu, 2011).
77 However, in the case of steam explosion a degradation of the hemicellulose was observed, which goes
78 paired with a reduction in water binding capacity of the plant cell wall and an increase in brittleness of
79 the structure (Ramos, 2003). These phenomena are more desired for the use of the treated biomasses in
80 power plants rather than for improving their texturizing properties in an aqueous system. Supercritical
81 CO₂ on the other hand shows promising results but still remains challenging in terms of cost
82 effectiveness.

83 The particle size reduction obtained during HPH is shown to go hand in hand with changes in
84 physicochemical properties but changes clearly depend on the microstructure of the plant material.
85 Significant increases in the WHC, the swelling capacity, the OHC and the CEC due to mechanical
86 processing were for example found for the insoluble fiber fraction of carrot pomace, for tomato paste
87 suspensions , and to a lesser extent for carrot suspensions, whereas no clear changes in the WHC of
88 apple sauce and potato pulp suspensions upon HPH were noticed (Chau et al., 2007; Bengtsson, &
89 Tornberg, 2011). The relation between changes in microstructural properties and changes in functional
90 properties due to HPH are however not yet completely understood.

91 The objective of the current work was to evaluate whether HPH could be used to functionalize orange
92 pulp. Hereto, orange pulp was homogenized using different pressure levels (200 and 800 bar) and the
93 resulting microstructural (particle size analysis and microscopy analysis) and functional properties (WHC,
94 swelling volume and rheological properties) were determined and compared to the initial orange pulp
95 properties. In order to evaluate the role of changes in cell wall polysaccharides in changes of functional
96 properties induced by HPH, the alcohol-insoluble residue (AIR) of the samples was analyzed in terms of
97 pectin extractability, degree of methyl-esterification (DME), neutral sugar composition and molar mass
98 distribution. In the second part of this work, subsamples with different particle size ranges were
99 prepared from the non-homogenized and the high-pressure homogenized orange pulp. These

100 subsamples were studied in terms of microstructural and functional properties in order to better
101 understand the functional properties of high-pressure homogenized orange pulp.

102

103 **2 Materials and methods**

104 **2.1 Orange pulp**

105 The orange pulp fibers were from Brazilian oranges, cultivar Valencia. They were from the 2010 harvest
106 and provided by Fischer S/A, a Brazilian orange juice company . The pulp, obtained after juice extraction,
107 was pasteurized for food safety reasons and for inactivation of intrinsically present pectin
108 methylesterase. The pulp was subsequently poured in 180 kg vessels and frozen. The vessels were
109 shipped by boat to Europe for the present study under frozen conditions. Moisture content of the
110 starting pulp was about 3.4%. The samples were thawed at ambient conditions to avoid structural
111 damage to the pulp, diluted to 2% dry matter content with standardized tap water (1.00 g NaCl and 0.15
112 g CaCl₂ in 1 L reverse osmosis water with a conductivity of 2.2±0.1 mS/cm at 25°C), blended and high-
113 pressure homogenized. The high-pressure homogenization was performed with a NS1001L-Panda 2k
114 equipped with a single R-valve (Niro Soavi). The R-valve, which is preferably used in the context of cell
115 rupture, consists of a cylindrical/flat type of impact head, a small impact ring and a passage head with
116 sharp angles. A homogenization condition commonly used in the food industry was used (200 bar) as
117 well as an elevated pressure level of 800 bar, which is a compromise between industrial process capacity
118 and the intended increased product functionality. Control samples, also further called ‘blended
119 samples’, underwent the same preparation procedure but no HPH step was applied in this case. Samples
120 were frozen with liquid N₂ and stored at -40°C until further analysis (after thawing at room
121 temperature).

122

123 **2.2 Isolation of the subsamples**

124 Orange pulp samples were loaded onto a wet-sieving column (Vibratory Sieve shaker AS200, Retsch) in
125 order to isolate relevant particle fractions, further called ‘subsamples’. Sieves with pore sizes of 250,
126 125, 80 and 40 µm were used. The material that was not retrieved on the smallest sieve (40 µm) was
127 centrifuged (30 min at 12500 g, Beckman Coulter centrifuge) in order to obtain subsamples that
128 contained the smallest material. The ranges that are used to refer to the different fractions are the pore
129 sizes of the sieves used during the isolation process.

130

131 2.3 Particle size analysis

132 The particle size distribution of the samples was analyzed by laser diffraction (Mastersizer, Malvern). A
133 refractive index of 1.56 was used for the cell wall particles. From the particle size analysis, different
134 diameters can be obtained: (i) $D(v, 0.1)$, $D(v, 0.5)$ and $D(v, 0.9)$ respectively represent the maximum
135 particle diameter below which 10%, 50% or 90% of the sample volume exists, (ii) $D[4,3]$ shows the
136 volume based mean diameter and (iii) $D[3,2]$ indicates the surface area based mean diameter.

137

138 2.4 Microscopy analysis

139 Microscopy pictures of diluted samples (~1:10) were taken using a light microscope (Olympus BX-41). In
140 addition, immunofluorescence using the pectin-specific antibody JIM7 was performed. Hereto, the
141 samples were incubated with the primary antibody JIM7 (fivefold diluted in phosphate buffered saline
142 containing 3% milk powder (MPBS); PlantProbes, Leeds, UK) for 1 h and 30 min at room temperature.
143 After primary labeling, samples were washed with PBS by centrifugation (3 times 5 min at 22 °C and 400
144 g; Microfuge 22R Centrifuge, Beckman Coulter, Germany). For the visualization of JIM7, secondary
145 labeling with an anti-rat Ig antibody coupled to fluorescein isothiocyanate (FITC) (Nordic Immunology,
146 Tilburg, The Netherlands) was used. The secondary antibody was diluted 1/20 in 3% MPBS. After a final
147 washing step with PBS, samples were mounted in an anti-fade agent (Citifluor, Agar Scientific, Stansted,
148 United Kingdom) on glass slides and examined with the Olympus BX-41 microscope equipped with
149 epifluorescence illumination. Immunolabeling experiments were carried out at least in duplicate.

150

151 2.5 Water holding capacity

152 The orange pulp fiber dispersions were diluted to a 1% concentration (on a dry weight basis) in
153 standardised tap water by using a 4-bladed propeller fitted on a RWD 20 digital IKA stirrer (set at 900
154 rpm for 10 min) in a 400 mL glass beaker with diameter of 7.8 cm. Subsequently, the dispersions were
155 transferred into 50 mL centrifuge tubes and centrifuged at 3500 g for 5 min. The WHC was calculated
156 from the gravimetric measurement of supernatant and packed hydrated fiber. All analyses were
157 performed in duplicate.

158

159 2.6 Swelling volume

160 The orange pulp fiber suspensions were diluted to a 1% concentration (on a dry weight basis) in
161 standardised tap water by using a 4-bladed propeller fitted on a RWD 20 digital IKA stirrer (set at 900
162 rpm for 10 min) in a 400 mL glass beaker with diameter of 7.8 cm. The dispersions were transferred into

163 100 mL graduated cylinders and the bed volume was recorded after 24 h (to the nearest 0.5 mL). All
164 measurements were performed in duplicate.

165

166 2.7 Rheological properties

167 Flow curves of the orange pulp samples were determined at 20.0 °C on a Physica MCR 301 rheometer
168 (Anton Paar GmbH, Graz, Austria) with a coaxial cylinder configuration (TEZ 150P), a symmetrical blades
169 spindle (ST24-2D/2V/2V-30, diameter 24 mm, total vane length 30 mm, top and medium blades are
170 vertical and crossed, bottom blades are aligned with top blades and tilted vertically by an angle of 45°)
171 and a profiled measuring cup (CC27/T200/SS/P, diameter 28.9 mm, 20 indents of 0.5 mm depth). Since
172 the rheological method was based on Debon et al. (2012), the pulp concentration of the samples was
173 adjusted before the measurement to the concentration validated in that study. Therefore, orange pulp
174 samples were centrifuged at 3500 g for 10 min and 4% fiber pellet was reconstituted with supernatant.
175 24 h after reconstitution, 40.0 (\pm 0.2) g fiber dispersion was presheared for 300 s at 100 s⁻¹ (to avoid the
176 effect of loading). Then, the shear rate was decreased in 20 steps from 100 to 1 s⁻¹ and the measuring
177 time increased logarithmically from 6 to 30 seconds. The flow curves were fitted with the Herschel-
178 Bulkley model. All measurements were performed in duplicate. As the amount of subsample was
179 limited, the flow curves of these samples could not been determined.

180 For both the orange pulp samples and subsamples, an oscillatory strain sweep test was carried out at
181 20.0 °C on a Physica MCR 301 rheometer (Anton Paar GmbH, Graz, Austria) with a parallel plate (PP25,
182 24.96 mm diameter, concentricity \pm 5 μ m, parallelity \pm 1 μ m) at 1 mm gap. Due to the limited amount of
183 subsample, both the orange pulp samples and subsamples were measured with a parallel plate
184 (although the rather large particle size of the samples) to allow comparison of the oscillatory data of
185 both sample types. After sample loading and trimming, the sample was equilibrated 20 min at 20 °C
186 under a Peltier hood. The strain was then increased in 60 steps from 0.1 to 100% and the measuring
187 time decayed logarithmically from 30 to 10 s. The angular frequency was set at 10 rad/s. All
188 measurements were performed in duplicate, 24 h after orange pulp fiber dispersion in standardised tap
189 water and centrifugation at 3500 g for 10 min.

190

191 2.8 Characterization of cell wall polysaccharides

192

193 2.8.1 The alcohol-insoluble residue

194 The cell wall material of orange pulp samples was isolated as alcohol-insoluble residue (AIR) according to
195 the method of McFeeters and Armstrong (1984). Approximately 10 g of the material was homogenized
196 in 64 mL 95% (v/v) ethanol using a mixer (Buchi mixer B-400, Flawil, Switzerland). The suspension was
197 filtered (Machery-Nagel MN 615 Ø 90 mm) and the residue was rehomogenized in 32 mL 95% (v/v)
198 ethanol. After another filtration step, the residue was homogenized in 32 ml acetone. A final filtration
199 resulted in the AIR, which was dried overnight at 40 °C. The AIR was ground using a mortar and pestle
200 and stored in a desiccator until further use.

201

202 2.8.2 Fractionation

203 According to the extractability with different media, the alcohol-insoluble cell wall material was
204 fractionated into different pectin-rich fractions and one hemicellulose-rich fraction. The water-
205 extractable pectin (WEP) fraction was obtained by incubating 0.5 g AIR in 90 mL boiling water while
206 stirring (Sila, Smout, Elliot, Van Loey, & Hendrickx, 2006). After 5 min, the suspension was cooled under
207 running tap water and filtered. The filtrate was collected and adjusted to 100 mL (WEP). The residue was
208 re-suspended in 90 mL 0.05 M cyclohexane-trans-1,2-diamine tetra-acetic acid (CDTA) in 0.1 M
209 potassium acetate (pH 6.5) for 6 h at 28 °C after which a new filtration step followed (Chin, Ali, & Hazan,
210 1999). After adjusting the filtrate volume to 100 mL, the chelator-extractable pectin (CEP) fraction was
211 obtained. The residue was re-incubated in 80 mL 0.05 M Na₂CO₃ containing 0.02 M NaBH₄ for 16 h at 4
212 °C, and subsequently for 6 h at 28 °C (Chin et al., 1999). The mixture was filtered and the volume of the
213 filtrate was adjusted to 100 mL, which resulted in the sodium carbonate-extractable pectin (NEP)
214 fraction. The residue was re-incubated under N₂ atmosphere in 90 mL of 4 M KOH, 0.02 M NaBH₄, and
215 3.5% borate for 22 h at room temperature. The suspension was filtered and the filtrate was adjusted to
216 200 mL after pH adjustment (pH 5.0) to obtain the hemicellulose fraction (HF). All fractions, including
217 the remaining residue, were frozen with liquid N₂ and stored at -40 °C until further analysis.

218

219 2.8.3 Uronic acid content

220 To determine the uronic acid (UA) content in the AIR and the WEP and the CEP fraction of the
221 (sub)samples, hydrolysis was performed with concentrated sulfuric acid according to the procedure by
222 Ahmed and Labavitch (1977). Briefly, 8 mL of concentrated H₂SO₄ (98 %) was added to 20 mg of AIR or to
223 2 mL of the liquid fraction, after which 2 mL of distilled water was added dropwise. The solution was
224 stirred for 5 min and another 2 mL of distilled water was added dropwise. The sample was stirred until it
225 was completely dissolved (4 h for AIR, 1 h for the fractions) and diluted to 50 mL or 25 mL for

226 respectively the AIR and the fractions. Then, the UA concentration was quantified using the
227 spectrophotometric method described by Blumenkrantz and Asboe-Hansen (1973), according to which
228 0.6 mL of the hydrolysate was heated (5 min at 100°C) in sodium borate (1:6; 0.0125 M sodium
229 tetraborate in 98% H₂SO₄). Subsequently, the solution was cooled down to room temperature and
230 mixed with metahydroxydiphenyl (60 µL of 0.15% metahydroxydiphenyl in 0.5% NaOH) after which the
231 absorbance was measured at 520 nm and 25 °C. The hydrolysis step was carried out in duplicate while
232 three colorimetric analyses were performed for each hydrolysate.

233

234 2.8.4 Pectin degree of methyl-esterification

235 The degree of methyl-esterification (DME) of pectin in AIR and in the WEP and the CEP fraction was
236 determined as the ratio of the molar amount of methyl-esters to the molar amount of UA residues. The
237 DME of NEP could not be assayed due to the saponification of methyl-esters during the alkali extraction
238 of this fraction.

239 To quantify the amount of methyl-esters, the ester bonds were saponified with NaOH according to the
240 procedure of Ng and Waldron (1997). Briefly, the samples (20 mg of AIR in 8 mL of distilled water or 8
241 mL of WEP and CEP) were saponified with 2 M NaOH (3.2 mL) for 1 h at 20 °C. The saponified samples
242 were subsequently neutralized by 2 M HCl (3.2 mL) and diluted to 25 mL (for WEP and CEP) or 50 mL (for
243 AIR) with a 0.0975 M phosphate buffer pH 7.5. The amount of methanol released was measured using
244 the spectrophotometric method of Klavons and Bennett (1986). In this procedure, methanol in 1 mL of
245 the hydrolysate was oxidized to formaldehyde with alcohol oxidase (Sigma-Aldrich, Bornem, Belgium) (1
246 ml of 1 unit/mL solution), followed by a condensation with 0.02 M 2,4-pentanedione in 0.2 M
247 ammonium acetate and 0.05 M acetic acid (2 mL; 15 min incubation at 58 °C) to 3,5-diacetyl-1,4-
248 dihydro-2,6-dimethylpyridine. This colored product was determined at 412 nm and 25°C. The hydrolysis
249 step was again carried out in duplicate while three colorimetric analyses were performed for each
250 hydrolysate.

251

252 2.8.5 Molar mass distribution

253 All pectin fractions (WEP, CEP and NEP) were lyophilized using a freeze-dryer (Christ alpha 2-4,
254 Osterode, Germany). Lyophilized WEP and NEP samples were dissolved in demineralized water (WEP:
255 0.25% w/v, NEP: 1.5% w/v) and extensively dialyzed against demineralized water during 48 h. CEP
256 samples were also dissolved in demineralized water (7.5% w/v), but dialyzed against 0.1 M NaCl during
257 24 h, followed by dialysis against demineralized water for another 24 h. The dialyzed pectin fractions

258 were adjusted to a concentration of 0.05 M NaNO₃ before analysis. The HF fraction was dialyzed against
259 water, lyophilized and dissolved (0.5% w/v) in 0.05 M NaNO₃.

260 The molar-mass (MM) distribution of the different fractions was analyzed by means of high-
261 performance size exclusion chromatography. This was achieved using an Akta Purifier (GE Healthcare,
262 Uppsala, Sweden) equipped with a mixed-bed column of TSK-GEL (GMPWXL, 300 mm x 7.8 mm, pore
263 size = 100-1000 Å, particle size = 13 µm, theoretical plates/column ≥ 7000, pH range = 2-12, maximum
264 pressure = 300 psi; Tosoh Bioscience, Stuttgart, Germany) in combination with a TSK guard column
265 (PWXL). A 20 µL injection loop was used. Elution was executed with 0.05 M NaNO₃ at a flow rate of 0.7
266 mL/min for 25 min at 35 °C. A Shodex RI-101 detector (Showa Denko K.K., Kawasaki, Japan) was used to
267 monitor the eluent. In order to enhance the clarity of presentation, the signal (mV) obtained by the
268 detector was normalized through dividing all data points by the peak signal. Pullulan standards with MM
269 ranging from 180 to 788000 Da (Varian Inc, Palo Alto, California) were eluted to estimate the MM of the
270 fractions.

271

272 2.8.6 Neutral sugar composition

273 Cell wall fractions (0.005 g of freeze-dried WEP, CEP, NEP or HF) were hydrolyzed with 0.5 mL 4 M
274 trifluoroacetic acid at 110 °C for 1.5 h. The digested samples were cooled, dried under N₂ at 45 °C,
275 neutralized with 0.25 mL 1 M NH₄OH, and dried again under N₂ at 45 °C. Before analysis of neutral
276 sugars, the samples were diluted to 5 mL with demineralized water (organic free, 18 MΩ cm resistivity),
277 supplied by a Simplicity™ water purification system (Millipore, Billerica, USA).

278 The monosaccharides were analyzed with HPAEC using a Dionex system (DX600), equipped with a GS50
279 gradient pump, a CarboPac™ PA20 column (150 x 3 mm), a CarboPac™ PA20 guard column (30 x 3 mm).
280 An ED50 electrochemical detector (Dionex, Sunnyvale, USA) equipped with a reference pH electrode
281 (Ag/AgCl) and a gold electrode was used in the pulsed amperometric detection mode, performing a
282 quadruple potential waveform. Potentials E₁ = 0.1 V, E₂ = -2.0 V, E₃ = 0.6 V, and E₄ = -0.1 V were applied
283 for duration times t₁ = 400 ms, t₂ + t₃ = 40 ms, and t₄ = 60 ms. Samples (10 µl) were injected and eluted
284 at a flow rate of 0.5 ml/min at 30 °C. Two separate gradients for each sample enabled a complete
285 chromatographic separation of the analyzed monosaccharides (Fuc, Rha, Ara, Gal, Glc, Xyl, Man). After
286 equilibration with 100 mM NaOH for 5 min and another 5 min with 15 mM or 0.5 mM NaOH (for
287 gradient 1 and gradient 2 respectively), samples were isocratically eluted using 15 mM or 0.5 mM NaOH
288 (for gradient 1 and gradient 2 respectively) during 20 min. Afterwards, the column was regenerated

289 using 500 mM NaOH for 10 min. Mixtures of commercial sugar standards (Fuc, Rha, Ara, Gal, Glc, Xyl,
290 Man) at concentrations of 1 to 10 ppm were used daily as external standards for identification and
291 quantification.

292 To correct for degradation of the monosaccharides during the acid hydrolysis step, recovery values were
293 estimated. Hereto, mixtures of the sugar standards were subjected to the aforementioned hydrolysis
294 conditions, and the peak areas were compared to those of untreated standard mixtures.

295

296 2.9 Statistical analysis

297 All functionality parameters were measured in duplicate. The hypothesis test for the difference in the
298 means of the populations is the unpaired samples t test (Rees, 1997). The level of significance was set at
299 $P < 0.05$.

300

301 **3 Results and discussion**

302

303 3.1 Effect of high-pressure homogenization on the microstructural and functional properties of 304 orange pulp

305 As a result of juice extraction, orange pulp consists of ruptured juice vesicles. These juice vesicles mainly
306 contain parenchyma tissue cells with a polysaccharide-rich (cellulose, hemicelluloses and pectin) cell
307 wall. In terms of composition, orange pulp is thus an ideal functional ingredient. Although the swelling
308 volume (88 mL/g) and WHC (23.9 g/g_{anh}) are relatively high, the rheological properties of orange pulp
309 dispersions under flow conditions (Table 1) can however be improved towards higher viscosity and yield
310 stress values. Moreover, the product is very coarse and quite heterogeneous.

311 HPH of orange pulp resulted in a more homogeneous suspension with a smoother appearance
312 compared to the blended orange pulp suspension, particularly in case of the 800 bar treated pulp. The
313 swelling volume and WHC of the 200 bar homogenized sample remained similar to the initial raw
314 material (Table 1). However, both the Herschel-Bulkley yield stress and consistency index (which gives
315 an idea on the viscosity of a fluid) greatly increased. The 800 bar suspension demonstrated a non-
316 significant increase in both swelling volume and WHC, while the changes in flow properties were rather
317 limited compared to the 200 bar treated sample (Table 1). The values found for the different samples
318 were significantly higher than previously reported (Debon, Wallecan, & Mazoyer, 2012). However, the
319 samples from the mentioned study had been dried after HPH treatment. This most likely resulted in

320 partial shrinkage and structural collapse of the fibers, which would explain the observed differences.
321 Similar observations were made on other dried plant cell wall systems (Kunzek, 2005).

322 The effect of HPH on the particle size distribution of orange pulp is given in Fig. 1. As expected, a clear
323 reduction in particle size upon HPH could be noticed. This reduction was moreover depending on the
324 pressure level, and hence the shear forces, applied: the average particle size (the $D [v, 0,5]$ value) of
325 blended orange pulp of 409 μm decreased to respectively 163 and 49 μm upon HPH at 200 and 800 bar.
326 The particle size reduction was also very clear from the microscopic observations (Fig. 2) showing large
327 tissue material in the blended sample going to completely distorted orange tissue material in the sample
328 homogenized at 800 bar. The observed changes are comparable to changes in particle size, linked to
329 changes in functional properties, for different other plant matrices (Chau et al., 2007; Bengtsson, &
330 Tornberg, 2011). It must however be emphasized that although particle size reduction during HPH can
331 be the main factor affecting the functional properties of plant-tissue based material, other changes like
332 for example changes in polysaccharides (see changes in pectin extractability in the second part of this
333 work), particle shape and particle rigidity might significantly contribute to the observed changes in
334 functional properties.

335

336 3.2 Effect of high-pressure homogenization on the cell wall polysaccharides in orange pulp

337 The cell wall material of blended and high-pressure homogenized orange pulp was extracted as AIR. As
338 expected, a high extraction yield (0.86 g AIR per g dry matter) was obtained (Table 2). The yield was
339 however shown to decrease upon HPH at elevated pressure (800 bar). Also the UA content of the
340 sample homogenized at 800 bar was lower (0.286 g UA per g dry matter) than the one obtained for the
341 blended sample (0.328 g UA per g dry matter) and the sample homogenized at 200 bar (0.322 g UA per g
342 dry matter) clearly indicating that HPH affects the amount of alcohol-insoluble material in orange pulp.

343 Hand in hand with these changes, changes in the pectin extractability properties upon HPH were
344 noticed: the AIR of the blended orange pulp only contained a small amount of WEP (14.2%) whereas the
345 AIR of the orange pulp homogenized at 800 bar contained more than 30% WEP. The data clearly show
346 that HPH at increasing pressure causes a gradual shift in the extractability properties of the pectic
347 polymers, making them less tightly bound to the orange pulp cell walls and thus more easily extractable.
348 The results moreover show that overall the amount of WEP gradually increases at the expense of the
349 NEP fraction, a fraction which is assumed to be rich in ester-bound pectin. This intriguing effect of HPH
350 on pectin extractability has been previously shown for carrot purées (Christiaens et al., 2012a) but was

351 not noticed for broccoli or tomato purée (Christiaens et al., 2012b; Christiaens et al. 2012c). In other
352 words, the effect is clearly matrix dependent but apparent in orange pulp.

353 In line with previous results on other matrices (Christiaens et al., 2012a/b/c), HPH did not affect the
354 DME of orange pulp AIR and the different fractions. Specifically, a DME of 62-69% was observed for
355 (homogenized) orange pulp AIR and CEP while a DME of 78-80% was noticed for (homogenized) orange
356 pulp WEP. On the other hand, the fractions' composition in terms of neutral sugars (Table 3) was
357 affected by the HPH treatment. Pectin polymers present in the WEP and CEP fraction of orange pulp
358 were shown to possess rather low amounts of neutral sugars compared to the amount of the backbone
359 UA units. A comparable ratio between neutral sugars and UA was found in tomato AIR which is known to
360 contain rather linear pectin polymers (Houben, Jolie, Fraeye, Van Loey, & Hendrickx, 2011). After HPH,
361 the ratio between UAs and neutral sugars was however changed for both the WEP and the CEP. Pectic
362 polymers in the WEP fraction of the high-pressure homogenized orange pulp were relatively richer in UA
363 compared to the blended sample, while the reverse effect was observed for the CEP. Also the
364 composition of the NEP, which is far more rich in rhamnogalacturonan-I-type neutral sugars, was
365 affected by HPH: due to HPH, the UA content in NEP is seriously decreased while the amount of neutral
366 sugars present only slightly decreased (for Rha and Ara) or even increased (Gal), indicating that HPH
367 affects the type of pectins (linear *versus* branched) present in the different fractions. After HPH, pectic
368 polymers in the WEP fraction are relatively richer in UA while the polymers in the CEP and the NEP
369 fractions become enriched in rhamnogalacturonan-I-type neutral sugars. These shifts are not surprising
370 as HPH changes the extractability characteristics of the pectic polymers in orange pulp and indicate that,
371 due to HPH, especially UA-rich pectic polymers are shifted from the CEP and/or NEP fractions to the
372 WEP fraction.

373 To investigate whether HPH also affected the size of the pectic polymers, the molar mass distribution of
374 the polymers in the different fractions was determined. HPH was clearly shown to decrease the size of
375 the pectic polymers in the WEP fraction: whereas the WEP of the blended sample has a molar mass
376 higher than 788 kDa, the WEP of the orange pulp high-pressure homogenized at 800 bar has a molar
377 mass around 404 kDa (Fig. 3). In addition, the molar mass distribution of the latter polymers was less
378 poly-disperse than the one of the blended sample. The molar mass and molar mass distribution of the
379 CEP (with an average molar mass higher than 788 kDa) and NEP (with a very broad molar mass
380 distribution between 47.3 and 788 kDa) were not affected by HPH. These results thus suggest a
381 mechanical, depolymerizing effect of HPH on the water-extractable pectic polymers in the AIR of orange

382 pulp or might point at a conformational change of the water-extractable pectic polymers upon HPH.
383 Similarly, molar mass changes of water-extractable carrot pectins due to HPH were also noticed by
384 Christiaens et al. (2012a). In this case, the effect of HPH was observed similar, but smaller, compared to
385 the effect of thermal processing on the water-extractable pectin. In addition, also the molar mass of
386 other polymers like β -glucan (Kivelä, Pitkänen, Laine, Aseyev, & Sontag-Strohm, 2010), guar gum,
387 hydroxyethylcellulose, sodium carboxymethylcellulose and sodium alginate (Villay et al., 2012) was
388 shown sensitive to HPH. In contrast, no effect on the molar mass of Arabic gum was found (Villay et al.,
389 2012). Apparently, the globular structure of polymers like Arabic gum prevents the depolymerizing or
390 conformational changing action of HPH.

391 In summary of this part of the current study, it can be concluded that HPH at elevated pressure clearly
392 affects the cell wall polymer properties in orange pulp. Through the mechanical action of HPH, orange
393 pulp cell wall polymers become more soluble resulting in less alcohol-insoluble material and resulting in
394 a duplication of the amount of WEP in the AIR. Due to HPH, the size of these water-extractable pectic
395 polymers is moreover decreased and the fraction becomes more enriched in UAs. As a consequence of
396 these observations, it is expected that the pectin concentration in the serum of the orange pulp
397 dispersion increases by HPH. As pectin concentration is known to influence the viscosity of plant-based
398 dispersions (Moelants et al., 2013b), this aspect might be important for the rheological properties of
399 high-pressure homogenized orange pulp dispersions.

400

401 3.3 The role of particle size on the functional properties of high-pressure homogenized orange pulp

402 In order to better understand the role of particle size on the functional properties of the orange pulp
403 samples, subsamples of different sizes were isolated from the blended and high-pressure homogenized
404 orange pulp dispersions. Subsamples that could be isolated in a substantial amount (Table 4) were
405 considered relevant and were further investigated in terms of microstructural and functional properties.
406 As HPH affects the particle size within the orange pulp dispersions, HPH obviously influenced the
407 presence of the different subsamples. Whereas the blended sample only contained less than 10% of
408 material in the smallest subsample ($< 40 \mu\text{m}$), more than 40% and 90% of the material turns up in this
409 fraction for the orange pulp homogenized at 200 and 800 bar respectively. This shift in particle fractions
410 confirms the fact that the degree of material disintegration is related to the pressure level, and hence
411 the shear forces applied, during HPH. It must hereby however be emphasized that the average size of
412 particles in subsamples (Table 5) is larger than the pore size of the sieves through which the particles

413 could pass and is thus larger than the number that is used to refer to the subsamples. Specifically, the
414 average particle size of the orange pulp subsamples can be presented as $D(v, 0.5)$, $D[4,3]$ and $D[3,2]$.
415 Similar trends in these three diameters between the different subsamples can be observed. However,
416 due to the dominant contribution of large particles to the volume-based average diameters such as $D(v,$
417 $0.5)$, $D[4,3]$, their values were larger as compared to $D[3,2]$, the surface-based average diameter. Also
418 the distribution of the particles within one subsample exceeds the difference between the pore sizes of
419 two consecutive sieves. These observations can be explained by the irregular shape and deformability of
420 the orange pulp particles and the inability of the laser diffraction technique used to capture these
421 properties as particle sizes were calculated assuming a spherical shape (Fig. 2 and Fig. 4). Similar
422 observations were made by Moelants et al. (2013a) who investigated the particle size distribution of
423 sieved carrot particles. During microscopic analysis of the different subsamples (Fig. 4), a remarkable
424 observation was done for the smallest subsample obtained from the orange pulp homogenized at 800
425 bar. The material of this subsample formed a kind of a hydrocluster or soft gel particle during the
426 analysis, i.e. while being 'squeezed' between the glass slide and the cover glass and thus while being
427 subjected to high local stresses. Conversely, this phenomenon was not apparent for the other
428 subsamples.

429 The determination of the UA content of the different subsamples (Table 4) indicated that part of the
430 pectic polymers were washed out during the wet sieving procedure that was used to produce the
431 subsamples. This washing-out effect is important to consider in the context of the functional properties
432 of the subsamples as interaction properties of particles might be affected.

433 The swelling properties of the fiber subsamples were all very high (Table 6). In general, values close to
434 100% were found for all the suspensions. This is significantly higher than the values measured on the
435 total samples (see Table 1). It might be concluded that the individual particle subsamples will arrange
436 differently than when blended together. Moreover, an increase of the homogenization pressure
437 resulted in particle subsamples with higher WHC, especially for the subsamples containing the smallest
438 material ($< 40 \mu\text{m}$) (Table 6). Furthermore, a clear trend was observed for the subsamples obtained from
439 orange pulp homogenized at 200 bar: the smaller the subsample particle size, the higher the WHC. In
440 particular, the particle fraction below $40 \mu\text{m}$ showed the highest WHC upon centrifugation. The higher
441 WHC of the smaller particle fractions may be related to the higher specific surface area of these small
442 particles. When comparing with the WHC value obtained for the entire 200 bar sample (Table 1), it

443 appears that the smallest particle subfraction has a dominant effect on the ability of the fiber to retain
444 water.

445 To investigate the rheological properties of the orange pulp samples and subsamples, oscillatory strain
446 tests were performed under controlled shear deformation on the packed material after centrifugation at
447 3500 g. Due to the limited amount of sample, a strain sweep but no additional frequency sweep was
448 measured. Since the samples are known to behave as gels, the values of the storage (G') and loss
449 modulus (G'') are independent of the angular frequency at which they are measured for strains within
450 the linear viscoelastic (LVE) region. Therefore, G' values were obtained from the strain sweep for a
451 particular strain within the LVE and reported in Table 7, for the original (total) fiber samples as well as
452 for the subsamples with a different particle size. A first interesting finding was that the large particle
453 subsamples had significantly higher G' values compared to the small particle ones. This observation is in
454 correspondence with results for jaboticaba and carrot pulp obtained by Sato and Cunha (2009) and
455 Moelants et al. (2013a) respectively, and was particularly evident for the subsamples isolated from the
456 orange pulp that was homogenized at 200 bar. In addition, G' of the total samples was smaller than the
457 moduli of the individual subfractions, with exception of G' of the smallest particle subsample isolated
458 from the orange pulp homogenized at 200 bar. This might indicate that even though some subsamples
459 have a much higher G' on their own, an antagonistic effect is observed when the different subfractions
460 are mixed. Similarly, Moelants et al. (2013a) observed lower G' values for carrot purée than G' of the
461 reconstituted subfractions. The larger width of the particle size distribution in carrot purée was
462 mentioned as possible explanation for this observation.

463 However, caution should be taken when analyzing the rheological data. The various subsamples were
464 not measured at the same moisture content due to their differences in WHC (Table 1 and 6). Therefore,
465 comparing the strain sweep curves of the samples can only be done on a relative basis. G' normalization
466 was applied by dividing the G' values with the linear viscoelastic range storage modulus as a function of
467 strain as applied by Adams, Frith, & Stokes (2004) for soft agar microgels. It is known that the maximum
468 strain within the linear viscoelastic range is inversely proportional to the particle size and the packed
469 material modulus. The greater ability of the softer particle network (as size decreases) to deform prior
470 to flow may be due to the interaction of the hydroclusters (3D packing and lubrication forces). Similar
471 behavior has been observed for soft agar microgels (Adams et al., 2004). Interestingly, the total orange
472 pulp sample homogenized at 200 bar had a very different behavior than its corresponding subsamples
473 (Fig. 5a). The overall sample turned out to be less deformable (indicated by the smaller critical strain)

474 than its constituent subfractions. Comparison between the normalized G' evolutions of the total
475 samples (Fig. 5b) showed that the starting material and the 200 bar sample behaved very similar. Visible
476 differences in smoothness could be observed. However, the 800 bar sample showed a more soft gel
477 behavior than the two other samples (indicated by the lower $\tan \delta$ value for the sample homogenized at
478 800 bar in Table 7), which is in line with the microscopic evaluations (Fig. 4). When comparing the mass
479 balances of the fractions, it appeared that although about 40-45% of particles present in the 200 bar
480 sample were smaller than $40 \mu\text{m}$ (Table 4), this amount proved to be insufficient to significantly alter the
481 overall rigidity of the suspension.

482

483 **4 Conclusion**

484 Results obtained within the current work clearly suggest that the functional properties of orange pulp
485 suspensions are largely related to particle size. Particles smaller than $40 \mu\text{m}$ were proven to substantially
486 contribute to the swelling properties, the water holding capacity and the soft gel behavior of the fiber
487 suspensions. High-pressure homogenization (HPH) was shown to affect the particle size distribution,
488 and hence the functional properties of orange pulp whereby a pressure level higher than the one usually
489 applied in food industry (200 bar) was necessary to obtain orange pulp with desired functional
490 properties. By applying a homogenization step at 800 bar, a more homogenous orange pulp suspension
491 with a smooth appearance and with increased water holding capacity and improved swelling and flow
492 properties was obtained. This observation was related to the abundant presence of largely disintegrated
493 orange pulp material (particles smaller than $40 \mu\text{m}$) that behaved like a softer particle network. In
494 addition to the particle reducing effect of HPH, also the effect of HPH on cell wall polymers might
495 contribute to the improved functional properties of high-pressure homogenized orange pulp. HPH was
496 found to mechanically affect the pectic polymers within the orange pulp cell walls thereby decreasing
497 their size or conformation and increasing their extractability properties and as a consequence also
498 increasing their presence in the serum of the orange pulp suspension. As pectin is a relatively rigid
499 polymer with lots of functional groups allowing interaction with water, these changes might indeed
500 contribute to the enhanced water holding and swelling capacity of high-pressure homogenized orange
501 pulp. The rheology of the subfractions did not correlate well with the behavior of the total sample, in
502 particular for the samples homogenized at 200 bar. Further research would be to study the packing
503 behavior of the various fractions in particular under shear, which might explain the observed
504 antagonistic effects.

505 Finally, it should be noted that the concentrations at which the functionalized fibers demonstrated high
506 swelling properties in water, which resulted in particle suspensions with a high yield stress, are too low
507 (around 2-4%) for enriching a food product with the fiber alone. However, it opens opportunities for
508 replacing label-unfriendly ingredients by natural alternatives.

509

510 **5 Acknowledgements**

511 We thank the Cargill Texturizing Systems and Cargill Global FIS Research organization for their support
512 and in particular Geert Maesmans and Didier Bonnet. Sandy Van Buggenhout and Stefanie Christiaens
513 are Postdoctoral Researchers, funded by the Research Foundation Flanders (FWO).

514

515 **6 References**

516 Adams, S., Frith, W.J., & Stokes, J.R. (2004). Influence of particle modulus on the rheological properties
517 of agar microgel suspensions. *Journal of Rheology*, *48*, 1195-1213.

518 Ahmed, A., & Labavitch, J.M. (1977). A simplified method for accurate determination of cell wall uronide
519 content. *Journal of Food Biochemistry*, *1*, 361-365.

520 Bengtsson, H., & Tornberg, E. (2011). Physicochemical characterization of fruit and vegetable fiber
521 suspensions. I: Effect of homogenization. *Journal of Texture Studies*, *42*, 268-280.

522 Blumenkrantz, N., & Asboe-Hansen, G. (1973). New method for quantitative determination of uronic
523 acids. *Analytical Biochemistry*, *54*, 484-489.

524 Chau, C., Wang, Y., & Wen, Y. (2007). Different micronization methods significantly improve the
525 functionality of carrot insoluble fibre. *Food Chemistry*, *100*, 1402-1408.

526 Chin, L.H., Ali, Z.M. & Lazan, H. (1999). Cell wall modifications, degrading enzymes and softening of
527 carambola fruit during ripening. *Journal of Experimental Botany*, *50*, 767-775.

528 Christiaens, S., Van Buggenhout, S., Chaula, D., Moelants, K., David, C. C., Hofkens, J., Van Loey, A. M., &
529 Hendrickx, M. E. (2012a). In situ pectin engineering as a tool to tailor the consistency and syneresis of
530 carrot puree. *Food Chemistry*, *133*, 146-155.

531 Christiaens, S., Mbong, V. B., Van Buggenhout, S., David, C. C., Hofkens, J., Van Loey, A. M., & Hendrickx,
532 M. E. (2012b). Influence of processing on the pectin structure-function relationship in broccoli puree.
533 *Innovative Food Science and Emerging Technologies*, 15, 57-65.

534 Christiaens, S., Van Buggenhout, S., Houben, K., Chaula, D., Van Loey, A. M., & Hendrickx, M. E. (2012c).
535 Unravelling process-induced pectin changes in the tomato cell wall: An integrated approach. *Food*
536 *Chemistry*, 132, 1534-1543.

537 Debon, S.J.J., Wallecan, J., & Mazoyer, J. (2012). A rapid rheological method for the assessment of the
538 high pressure homogenization of citrus pulp fibers. *Applied Rheology*, 22, 63919-63930.

539 Hauner, H., Bechthold, A., Boeing, H., Brönstrup, A., Buyen, E., Leschik-Bonnet, E., Linseisen, J., Schulze,
540 M., Strohm, D., & Wolfram, G. (2012). Evidence-based guideline of the German nutrition society:
541 Carbohydrate intake and prevention of nutrition-related diseases. *Annals of Nutrition and Metabolism*,
542 60, 1-58.

543 Houben, K., Jolie, R., Fraeye, I., Van Loey, A.M., & Hendrickx, M.E. (2011). Comparative study of the cell
544 wall composition of broccoli, carrot and tomato: Structural characterization of the extractable pectins
545 and hemicelluloses. *Carbohydrate Research*, 346, 1105-1111.

546 Kivelä, R., Pitkänen, L., Laine, P., Aseyev, V., & Sontag-Strohm, T. (2010). Influence of homogenization on
547 the solution properties of oat β -glucan. *Food Hydrocolloids*, 24, 611-618.

548 Klavons, J.A., & Bennett, R.D. (1986). Determination of methanol using alcohol oxidase and its
549 application to methyl-ester content of pectins. *Journal of Agricultural and Food Chemistry*, 34, 597-599.

550 Kunzek, H. (2005). Hydratationseigenschaften von Zellwandmaterial und Ballaststoffen. *Deutsche*
551 *Lebensmittel-Rundschau*, 6, 238-255.

552 McFeeters, R.F., & Armstrong, S.A. (1984). Measurement of pectin methylation in plant cell walls.
553 *Analytical Biochemistry*, 139, 212-217.

554 Moelants, K.R.N., Cardinaels, R., Jolie, R.P., Verrijssen, T.A.J., Van Buggenhout, S., Zumalacarregui, L.M.
555 Van Loey, A.M., Moldenaers, P., & Hendrickx, M. (2013a). Relation between particle properties and
556 rheological characteristics of carrot-derived suspensions. *Food and Bioprocess Technology*, 6, 1127-
557 1143.

558 Moelants, K.R.N., Jolie, R. P., Palmers, S. K. J., Cardinaels, R., Christiaens, S., Van Buggenhout, S., Van
559 Loey, A. M., Moldenaers, P., & Hendrickx, M. (2013b). The effects of process-induced pectin changes on
560 the viscosity of carrot and tomato sera. *Food and Bioprocess Technology*, *6*, 2870-2883.

561 Narayanaswamy, A., Faik, A., Goetz, D.J., & Gu, T. (2011). Supercritical carbon dioxide pretreatment of
562 corn stover and switchgrass for lignocellulosic ethanol production. *Bioresource Technology*, *102*, 6995-
563 7000.

564 Ng, A., & Waldron, K.W. (1997). Effect of cooking and pre-cooking on cell-wall chemistry in relation to
565 firmness of carrot tissues. *Journal of the Science of Food and Agriculture*, *73*, 503-512.

566 Ramos, L.P. (2003). The chemistry involved in the steam treatment of lignocellulosic materials. *Quimica*
567 *Nova*, *26*, 863-871.

568 Rees, D. (1997). Essential statistics, Chapman & Hall, London.

569 Sato, A.C.K., & Cunha, R.L. (2009). Effect of particle size on rheological properties of jaboticaba pulp.
570 *Journal of Food Engineering*, *91*, 566-570.

571 Sila, D.N., Smout, C., Elliot, F., Van Loey, A., & Hendrickx, M. (2006). Non-enzymatic depolymerization of
572 carrot pectin: Toward a better understanding of carrot texture during thermal processing. *Journal of*
573 *Food Science*, *71*, E1-E9.

574 Tanashashi, M. (1990). Characterization and degradation mechanisms of wood components by steam
575 explosion and utilization of exploded wood. *Wood Research*, *77*, 49-117.

576 Villay, A., Lakkis de Filippis, F., Picton, L., Le Cerf, D., Vial, C., & Michaud, P. (2012). Comparison of
577 polysaccharide degradations by dynamic high-pressure homogenization. *Food Hydrocolloids*, *27*, 278-
578 286.

579 World Health Organization (2003). Diet, nutrition and the prevention of chronic diseases. In Report of a
580 Joint WHO/FAO Expert Consultation. WHO Technical Report Series, vol. 916. Geneva: World Health
581 Organization.

582

583 **5 Figure captions**

584 **Fig. 1** Particle size distribution curves of blended orange pulp and orange pulp high-pressure
585 homogenized at 200 bar and 800 bar.

586 **Fig. 2** Representative micrographs (1st row: bright field; 2nd row: labelled with JIM7) of blended and high-
587 pressure homogenized (at 200 and 800 bar) orange pulp.

588 **Fig. 3** Molar mass distribution of the WEP fraction in blended and high-pressure homogenized (at 200
589 bar and at 800 bar) orange pulp. Elution times of pullulan standards are indicated to allow for a rough
590 estimation of the molar mass.

591 **Fig. 4** Representative pictures (1st row: bright field; 2nd row: labelled with JIM7) of the '<40 μm '
592 subsample of blended and high-pressure homogenized (at 200 bar and 800 bar) orange pulp.

593 **Fig. 5** Normalized G' as function of strain for the different particle fractions obtained after 200 bar
594 homogenization (a) and for the total samples at 0 bar, 200 bar and 800 bar (b).

595 **Table 1.** Swelling volume, water holding capacity and Herschel-Bulkley parameters (\pm standard deviation; n = 2, from 2 separate pouches) of
 596 blended and high-pressure homogenized (at 200 bar and 800 bar) orange pulp fibers in standardised tap water.

	blended	200 bar	800 bar
Swelling volume (mL/g, dry weight basis) 1 g	88.0 (± 2.0) ^a	89.0 (± 2.4) ^a	94.0 (± 3.0) ^a
Water holding capacity (g water/g dry weight fiber) 3500 g	23.9 (± 0.9) ^a	23.6 (± 0.9) ^a	25.5 (± 0.1) ^a
Hershel-Bulkley fit at 4% concentration (dry weight basis)			
Yield stress (Pa)	99.3 (± 0.1) ^b	160.9 (± 10.6) ^a	183.7 (± 16.6) ^a
Consistency index (Pa.s)	70.8 (± 2.1) ^b	89.9 (± 1.4) ^a	66.4 (± 15.2) ^{a,b}
Pseudoplasticity Index (-)	0.275 (± 0.003) ^a	0.220 (± 0.001) ^b	0.237 (± 0.029) ^{a,b}
r ² of fit of each replicate	0.99625 0.99530	0.99993 0.99993	0.99957 0.99980

597 ^a measurements within a row with the same superscript letter are not significantly different (95% confidence limit).

598

599 **Table 2.** Alcohol-insoluble residue (AIR) content, uronic acid (UA) content (\pm standard deviation; n = 2) and the relative amount of the different
 600 fractions (UA in the fraction relative to UA in the sum of fractions \pm standard deviation; n = 2) in blended and high-pressure homogenized (at 200
 601 and 800 bar) orange pulp.

	AIR content	UA content	Pectin fraction (%)		
	(g AIR/g DM)	(g UA/g DM)	WEP	CEP	NEP
Blended	0.86 ± 0.02	0.328 ± 0.006	14.2 ± 0.3	37.0 ± 0.4	45.7 ± 0.8
200 bar	0.87 ± 0.02	0.322 ± 0.017	22.2 ± 0.5	36.8 ± 1.8	38.6 ± 1.4
800 bar	0.78 ± 0.03	0.286 ± 0.011	30.4 ± 1.2	36.3 ± 0.5	31.8 ± 0.7

602 *DM: dry matter*

603

604

605 **Table 3.** Neutral sugar content (mg/g AIR) (\pm standard deviation; n = 2) of pectic fractions, compared to the uronic acid (UA) content, in blended
 606 and high-pressure homogenized (at 200 and 800 bar) orange pulp (Fuc = fucose, Rha = rhamnose, Ara = arabinose, Gal = galactose, Glc = glucose,
 607 Xyl = xylose, Man = mannose).

		Fuc	Rha	Ara	Gal	Glc	Xyl	Man	UA*
Blended	WEP	0.20 \pm 0.01	1.75 \pm 0.14	6.10 \pm 0.30	5.18 \pm 0.26	2.99 \pm 0.15	1.21 \pm 0.02	1.62 \pm 0.08	46 \pm 1
	CEP	0.24 \pm 0.03	1.39 \pm 0.25	9.20 \pm 0.48	2.85 \pm 0.12	0.49 \pm 0.03	0.42 \pm 0.05	0.32 \pm 0.02	119 \pm 3
	NEP	0.84 \pm 0.12	8.47 \pm 0.02	55.18 \pm 5.28	23.00 \pm 4.07	3.01 \pm 2.64	13.30 \pm 16.05	4.98 \pm 5.98	147 \pm 3
200 bar	WEP	0.29 \pm 0.01	2.35 \pm 0.08	8.77 \pm 0.19	7.94 \pm 0.54	3.36 \pm 0.39	1.48 \pm 0.06	1.73 \pm 0.03	65 \pm 2
	CEP	0.23 \pm nd	1.45 \pm nd	9.36 \pm nd	3.00 \pm nd	0.46 \pm nd	0.46 \pm nd	0.31 \pm nd	108 \pm 6
	NEP	0.71 \pm 0.04	8.02 \pm 0.00	49.11 \pm 0.47	19.12 \pm 0.12	0.87 \pm 0.05	2.07 \pm 0.12	0.40 \pm 0.08	113 \pm 3
800 bar	WEP	0.25 \pm 0.05	1.96 \pm 0.55	8.81 \pm 1.61	6.25 \pm 1.58	1.74 \pm 0.34	0.94 \pm 0.34	0.87 \pm 0.25	81 \pm 10
	CEP	0.26 \pm 0.01	2.05 \pm 0.03	12.80 \pm 0.11	3.97 \pm 0.01	0.06 \pm 0.00	0.47 \pm 0.00	0.44 \pm 0.02	97 \pm 5
	NEP	1.38 \pm 0.00	6.58 \pm 0.78	46.55 \pm 0.98	24.60 \pm 2.69	2.03 \pm nd	6.94 \pm nd	1.28 \pm nd	85 \pm 2

608 * Colorimetrically determined

609 nd: not determined

610

611 **Table 4.** Approximate relative presence (weight %) of subsamples in blended and high-pressure homogenized (at 200 bar and 800 bar) orange
 612 pulp and uronic acid content (\pm standard deviation; n =2) in relevant subsamples.

		< 40 μ m	40-80 μ m	80-125 μ m	125-250 μ m
Blended	Relative presence (w %)	< 10%	< 10%	< 10%	\pm 15%
	UA content (g UA/g DM)	nd	nd	nd	0.251 ± 0.008
200 bar	Relative presence (w %)	> 40%	\pm 20%	\pm 20%	\pm 15%
	UA content (g UA/g DM)	0.238 ± 0.005	0.269 ± 0.007	0.271 ± 0.006	0.289 ± 0.002
800 bar	Relative presence (w %)	> 90%	\pm 8%	\pm 2%	-
	UA content (g UA/g DM)	0.250 ± 0.006	nd	nd	nd

613 DM: dry matter

614 nd: not determined

615

616 **Table 5.** Overview of particle size distribution parameters (and their standard deviation; n=2) for relevant subsamples obtained for the
 617 blended and high-pressure homogenized (at 200 bar and 800 bar) orange pulp.
 618

		D(v, 0.1)	D(v, 0.5)	D(v, 0.9)	D[4,3]	D[3,2]	Spread
Blended	125-250 µm	137.3	317.6	591.1	341.9	176.4	2.6
		<i>2.5</i>	<i>4.7</i>	<i>3.3</i>	<i>3.7</i>	<i>1.9</i>	<i>0.0</i>
200 bar	< 40 µm	16.9	51.2	123.7	63.3	26.0	4.1
		<i>0.4</i>	<i>1.1</i>	<i>10.9</i>	<i>4.7</i>	<i>0.0</i>	<i>0.4</i>
200 bar	40-80 µm	42.9	101.4	209.3	115.2	64.6	2.6
		<i>0.3</i>	<i>0.1</i>	<i>5.9</i>	<i>1.9</i>	<i>0.1</i>	<i>0.1</i>
200 bar	80-125 µm	61.1	152.4	314.6	172.9	92.0	2.8
		<i>0.1</i>	<i>0.6</i>	<i>3.8</i>	<i>1.4</i>	<i>0.4</i>	<i>0.0</i>
200 bar	125-250 µm	106.8	279.8	582.9	314.1	153.6	3.1
		<i>0.7</i>	<i>1.5</i>	<i>12.4</i>	<i>3.6</i>	<i>0.0</i>	<i>0.1</i>
800 bar	< 40 µm	13.3	39.4	100.9	52.3	21.7	4.0
		<i>0.7</i>	<i>1.8</i>	<i>17.7</i>	<i>8.7</i>	<i>0.2</i>	<i>0.7</i>

619

620

621

622 **Table 6.** Swelling volume and water holding capacity (\pm standard deviation; n = 2 from 2 separate pouches) of orange pulp fractions at 0 bar, 200
 623 bar and 800 bar in standardised tap water. Values in bold were obtained from a single measurement due to insufficient sample quantity to
 624 perform the evaluations in duplicate.

Batches orange pulp	blended	200 bar	200 bar	200 bar	200 bar	800 bar
	125-250 μm	125-250 μm	80-125 μm	40-80 μm	<40 μm	<40 μm
Swelling volume (mL/g, dry weight basis) 1 g	nps	95	nps	99 (± 1)	nps	nps
Water holding capacity (g water/g dry weight fiber) 3500 g	21.7	21.4	21.9 (± 0.2) ^c	22.6 (± 0.1) ^c	24.0 (± 0.2) ^b	27.3 (± 0.2) ^a

625 nps: no phase separation

626 ^a measurements within a row with the same superscript letter are not significantly different (95% confidence limit).

627

628

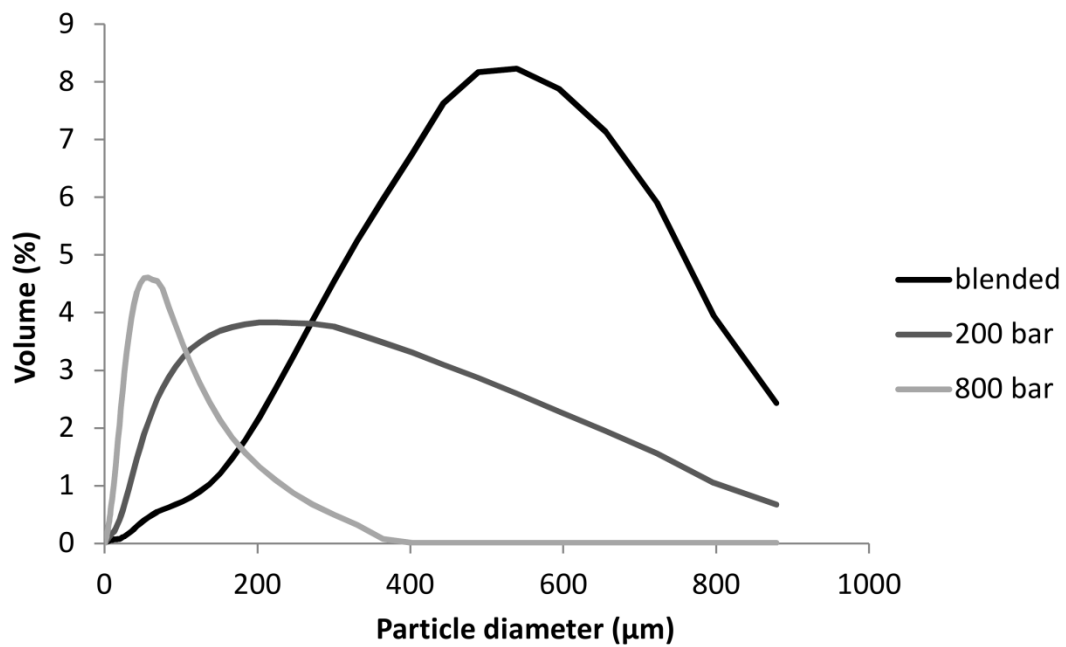
629 **Table 7.** Linear viscoelastic range moduli of the packed phase material after centrifugation at 3500 g.

Batches orange pulp	blended	blended	200 bar	200 bar	200 bar	200 bar	200 bar	800 bar	800 bar
	Total	125-250 μm	Total	125-250 μm	80-125 μm	40-80 μm	<40 μm	Total	<40 μm
G^* (Pa)	9977	13 640	5020	20 000	10 597	8 329	4 387	3212	4 367
G' (Pa)	9758	13 373	4930	19 807	10 499	8 245	4 337	3170	4 335
G'' (Pa)	2078	2 755	942	2 812	1 433	1 175	664	517	535
$\tan(\delta)$	0.21	0.21	0.19	0.14	0.14	0.14	0.15	0.16	0.12
LVR strain (%)	0.44	1.19	0.76	0.60	0.80	1.03	1.22	1.08	1.18

630

631

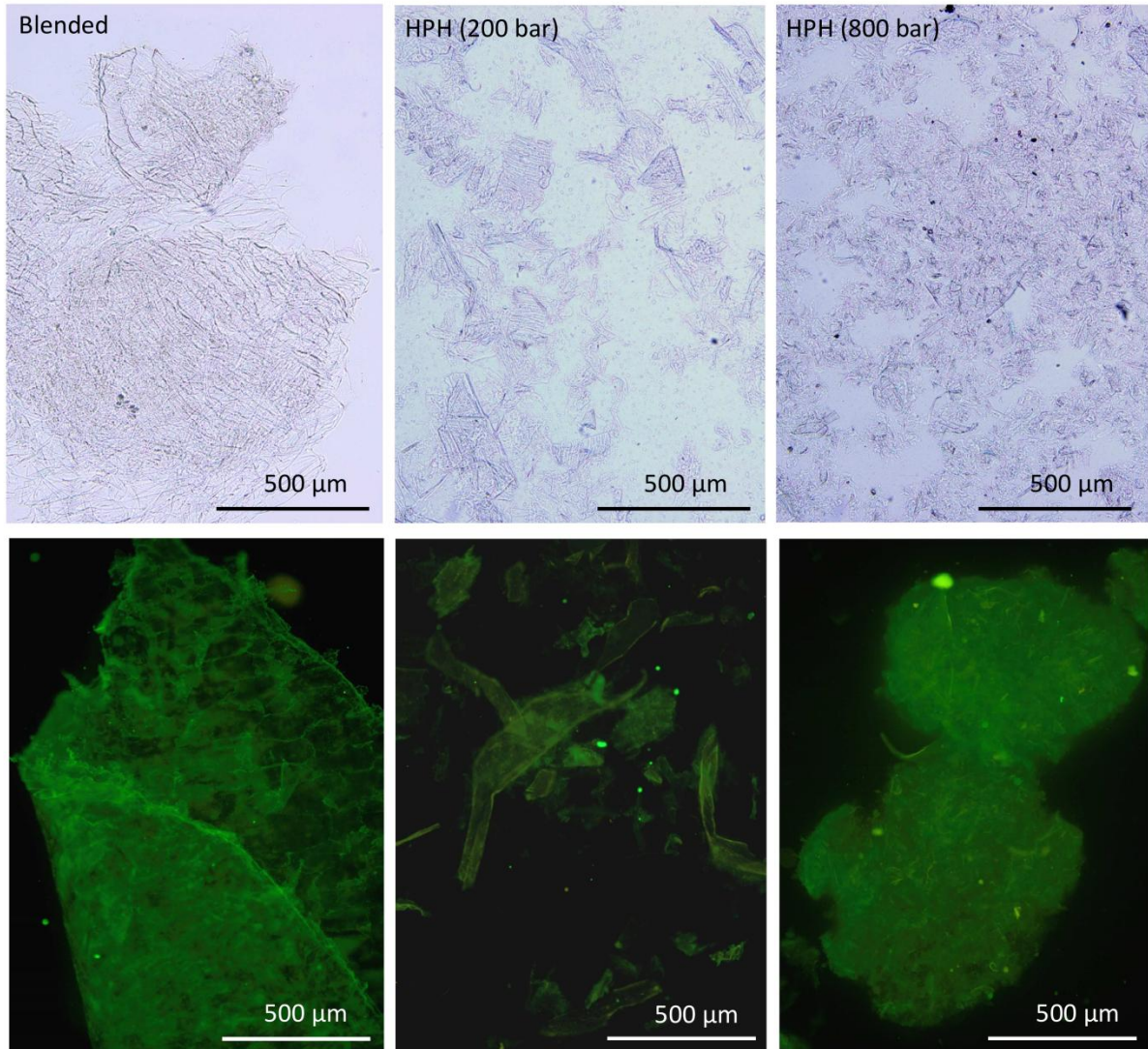
632



633

634 Figure 1

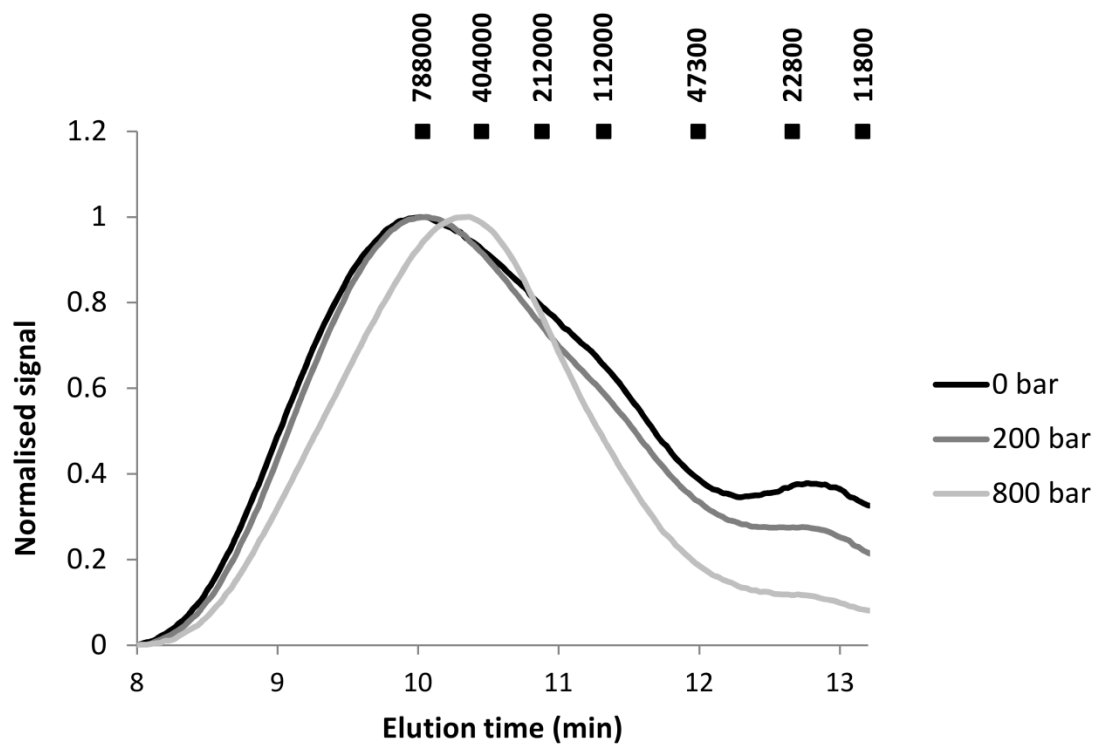
635



636

637 Figure 2

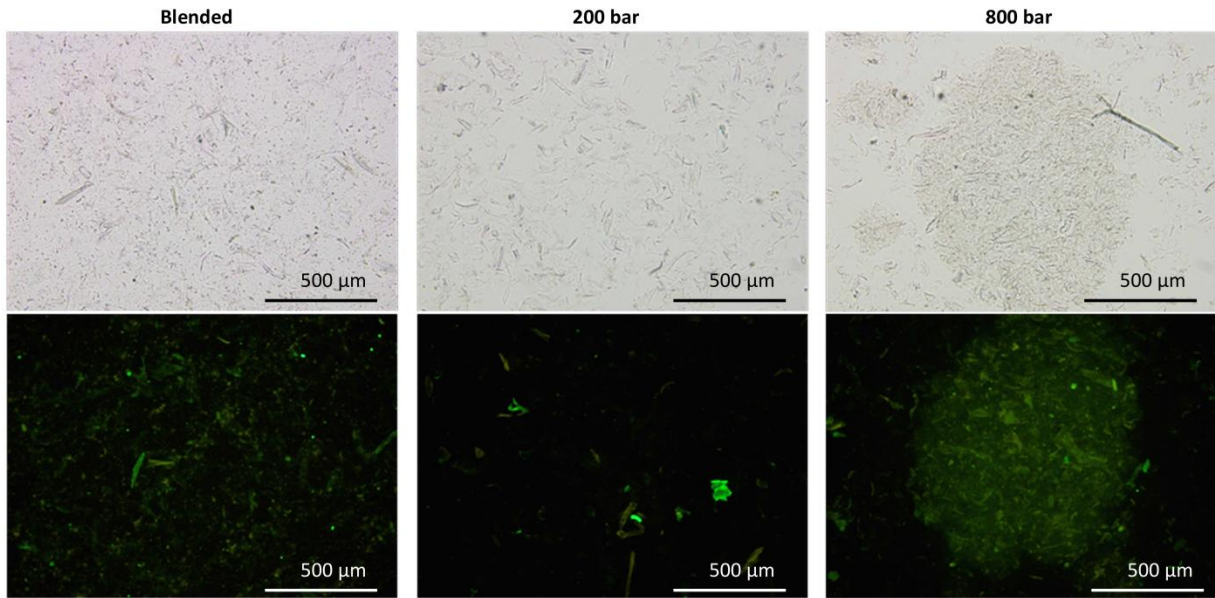
638



639

640 Figure 3

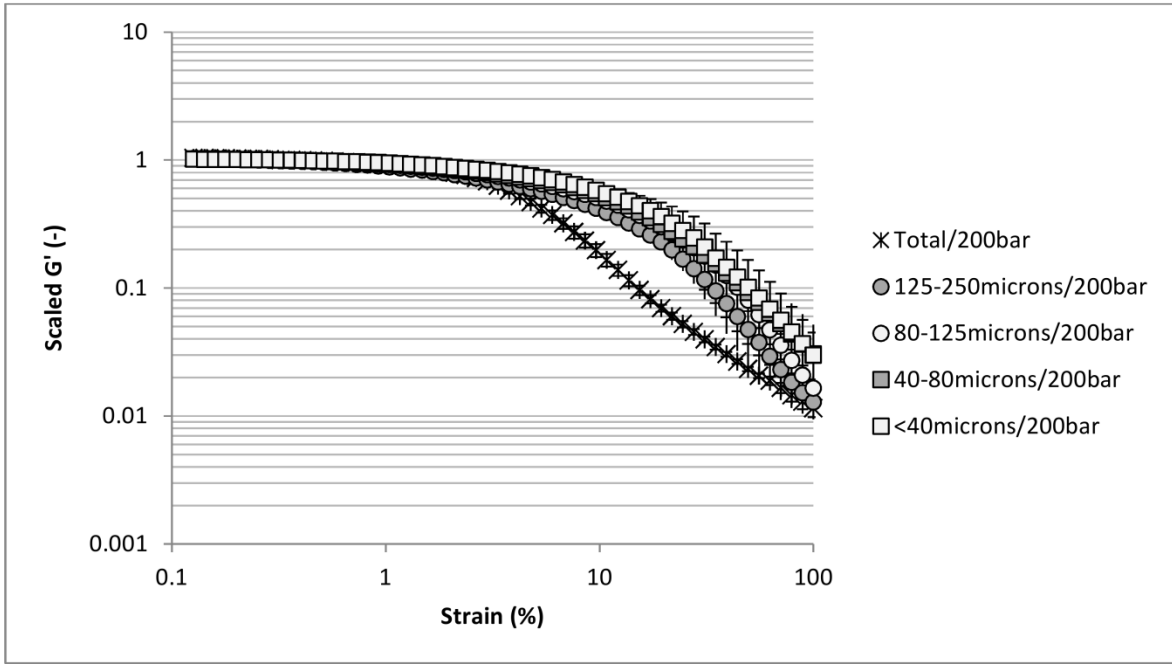
641



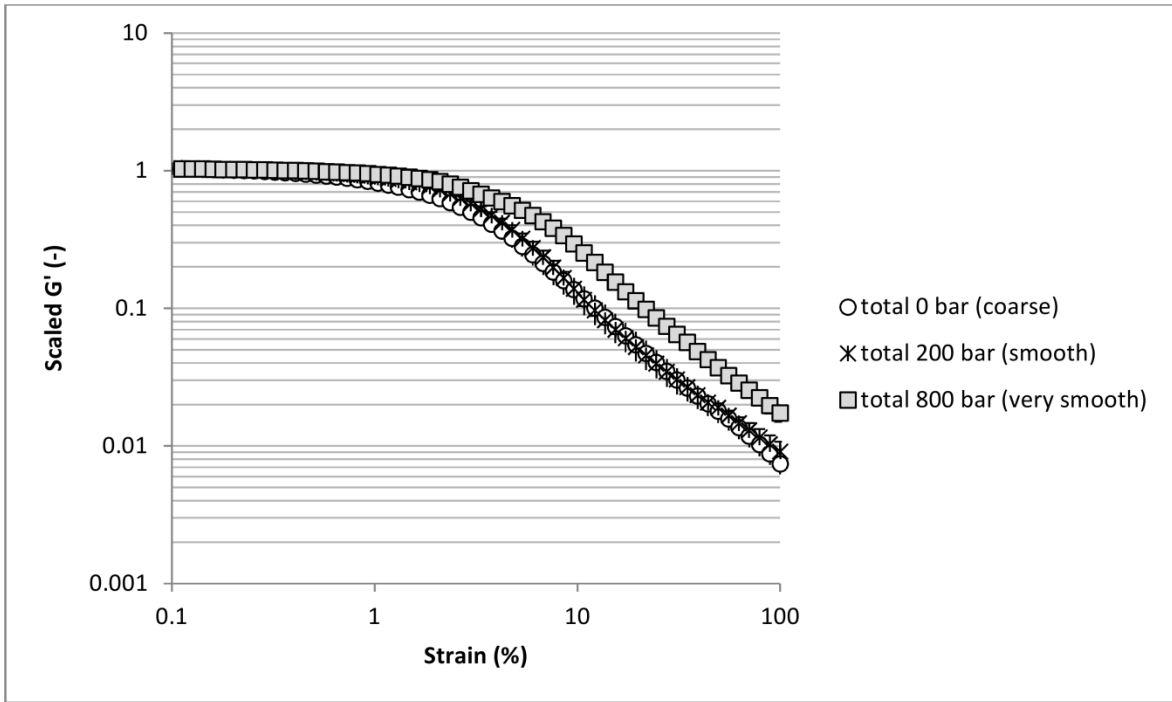
642

643 Figure 4

644



a



b

645

646 Figure 5

647